(fig. S20), the mechanical properties of the synthetic nacre are still not as good as that of natural nacre (*35*, *36*) (Fig. 4, B and C). Due to the larger aspect ratio of the aragonite platelets in the synthetic nacre, the platelets exhibit a "partly pullout" behavior, which leads to lower crack-resistance capability.

Because the precipitation of the second phase onto the matrix relies on electrostatic force, $CaCO_3$ and chitin can be substituted by other precursors with opposite charges to make superior composites such as engineering ceramics (*21*–*24*) (figs. S21 and S22). Besides, as the dependence of properties of the composite materials on the characteristic length of their periodic microstructure (*37*), the mechanical performance of these materials can be optimized by adjusting the properties of the original matrix (*38*), which affect both the amount of electrostatically absorbed precipitates and the density of the nucleation sites. The fabrication of the laminated synthetic nacre is not a special case; there are other techniques, such as programmable 3D printing, for constructing predesigned macroscopic matrices that can be readily incorporated with our strategy to produce composite materials. Moreover, this strategy is also adaptable for fabricating robust bulk materials with brittle and heat-labile components (fig. S21B). Given the importance of nano- and microscopic structures for the materials performance, we thus anticipate that our method can be extended to produce various composite materials with unique properties.

REFERENCES AND NOTES

1. P. Fratzl, R. Weinkamer, *Prog. Mater. Sci.* **52**, 1263–1334 (2007).
2. B. Ji, H. Gao, *Annu. Rev. Mater. Res.* **40**, 77–100 (2010).
3. J. Wang, Q. Cheng, Z. Tang, *Chem. Soc. Rev.* **41**, 1111–1129 (2012).
4. M. A. Meyers, J. McKittrick, P.-Y. Chen, *Science* **339**, 773–779 (2013).
5. H.-B. Yao, J. Ge, L.-B. Mao, Y.-X. Yan, S.-H. Yu, *Adv. Mater.* **26**, 163–188 (2014).
6. A. G. Checa, J. H. E. Cartwright, M.-G. Willinger, *Proc. Natl. Acad. Sci. U.S.A.* **106**, 38–43 (2009).
7. L. Addadi, D. Joester, F. Nudelman, S. Weiner, *Chemistry* **12**, 980–987 (2006).
8. Z. Huang, X. Li, *Sci. Rep.* **3**, 1693 (2013).
9. P.-Y. Chen *et al.*, *J. Mech. Behav. Biomed.* **1**, 208–226 (2008).
10. I. Jäger, P. Fratzl, *Biophys. J.* **79**, 1737–1746 (2000).
11. R. O. Ritchie, *Nat. Mater.* **10**, 817–822 (2011).
12. U. G. K. Wegst, H. Bai, E. Saiz, A. P. Tomsia, R. O. Ritchie, *Nat. Mater.* **14**, 23–36 (2015).
13. Z. Tang, N. A. Kotov, S. Magonov, B. Ozturk, *Nat. Mater.* **2**, 413–418 (2003).
14. A. Finnemore *et al.*, *Nat. Commun.* **3**, 966 (2012).
15. Y. Kim *et al.*, *Nature* **500**, 59–63 (2013).
16. T. Kato, T. Suzuki, T. Irie, *Chem. Lett.* **29**, 186–187 (2000).
17. L. J. Bonderer, A. R. Studart, L. J. Gauckler, *Science* **319**, 1069–1073 (2008).
18. P. Laaksonen *et al.*, *Angew. Chem. Int. Ed.* **50**, 8688–8691 (2011).
19. P. Das *et al.*, *Nat. Commun.* **6**, 5967 (2015).
20. B. Zhu *et al.*, *Angew. Chem. Int. Ed.* **54**, 8653–8657 (2015).
21. H. Le Ferrand, F. Bouville, T. P. Niebel, A. R. Studart, *Nat. Mater.* **14**, 1172–1179 (2015).
22. S. Deville, E. Saiz, R. K. Nalla, A. P. Tomsia, *Science* **311**, 515–518 (2006).
23. E. Munch *et al.*, *Science* **322**, 1516–1520 (2008).
24. F. Bouville *et al.*, *Nat. Mater.* **13**, 508–514 (2014).
25. H. Bai, Y. Chen, B. Delattre, A. P. Tomsia, R. O. Ritchie, *Sci. Adv.* **1**, e1500849 (2015).
26. F. Zhu *et al.*, *Chem. Asian J.* **8**, 3002–3009 (2013).
27. M. Niederberger, H. Cölfen, *Phys. Chem. Chem. Phys.* **8**, 3271–3287 (2006).
28. H. Cölfen, M. Antonietti, *Mesocrystals and Nonclassical Crystallization* (Wiley, Chichester, UK, 2008).
29. J. Wang, L. L. Shaw, *Biomaterials* **30**, 6565–6572 (2009).
30. D. Gebauer, H. Cölfen, A. Verch, M. Antonietti, *Adv. Mater.* **21**, 435–439 (2009).
31. S. Weiner, L. Addadi, H. D. Wagner, *Mater. Sci. Eng. C* **11**, 1–8 (2000).
32. J. Seto *et al.*, *Proc. Natl. Acad. Sci. U.S.A.* **109**, 3699–3704 (2012).
33. Y. Shao, H. P. Zhao, X. Q. Feng, H. Gao, *J. Mech. Phys. Solids* **60**, 1400–1419 (2012).
34. F. Barthelat, H. Tang, P. Zavattieri, C. Li, H. Espinosa, *J. Mech. Phys. Solids* **55**, 306–337 (2007).
35. R. Z. Wang, Z. Suo, A. G. Evans, N. Yao, I. A. Aksay, *J. Mater. Res.* **16**, 2485–2493 (2001).
36. R. Rabiei, S. Bekah, F. Barthelat, *Acta Biomater.* **6**, 4081–4089 (2010).
37. P. Fratzl, O. Kolednik, F. D. Fischer, M. N. Dean, *Chem. Soc. Rev.* **45**, 252–267 (2016).
38. S. Deville, *Adv. Eng. Mater.* **10**, 155–169 (2008).

ACKNOWLEDGMENTS

The authors thank Y. Tian, L. Chen, and Y. Guan for computed tomography imaging, and L. Wang for sample preparation. The authors also thank Y. Ni and Z. Song for discussion about mechanical models. This work was supported by the National Natural Science Foundation of China (grant 21431006), the Foundation for Innovative Research Groups of the National Natural Science Foundation of China (grant 21521001), the National Basic Research Program of China (grants 2014CB931800 and 2013CB931800), the Users with Excellence and Scientific Research Grant of Hefei Science Center of CAS (2015HSC-UE007 and 2015SRG-HSC038), and Key Research Program of Frontier Sciences, CAS (Grant QYZDJ-SSW-SLH036). Data are available in the supplementary materials.

SUPPLEMENTARY MATERIALS

www.sciencemag.org/content/354/6308/107/suppl/DC1
Materials and Methods
Figs. S1 to S22
Table S1
Movies S1 to S3
References (*39*–*49*)

17 April 2016; accepted 4 August 2016
Published online 18 August 2016
10.1126/science.aaf8991

COGNITION

Great apes anticipate that other individuals will act according to false beliefs

Christopher Krupenye,[1]*† Fumihiro Kano,[2,3]*† Satoshi Hirata,[2] Josep Call,[4,5] Michael Tomasello[5,6]

Humans operate with a "theory of mind" with which they are able to understand that others' actions are driven not by reality but by beliefs about reality, even when those beliefs are false. Although great apes share with humans many social-cognitive skills, they have repeatedly failed experimental tests of such false-belief understanding. We use an anticipatory looking test (originally developed for human infants) to show that three species of great apes reliably look in anticipation of an agent acting on a location where he falsely believes an object to be, even though the apes themselves know that the object is no longer there. Our results suggest that great apes also operate, at least on an implicit level, with an understanding of false beliefs.

Central to everything that makes us human—including our distinctive modes of communication, cooperation, and culture—is our theory of mind (TOM). TOM is the ability to impute unobservable mental states, such as desires and beliefs, to others (*1*, *2*). For nearly four decades, a cardinal question in psychology has concerned whether nonhuman animals, such as great apes, also possess this cognitive skill (*1*, *3*). A variety of nonverbal behavioral experiments have provided converging evidence that apes can predict others' behavior, not simply based on external cues but rather on an understanding of others' goals, perception, and knowledge (*3*, *4*). However, it remains unclear whether apes can comprehend reality-incongruent mental states (e.g., false beliefs) (*3*), as apes have failed to make explicit behavioral choices that reflect false-belief understanding in several food-choice tasks (*4*–*6*). False-belief understanding is of particular interest because it requires recognizing that others' actions are driven not by reality but by beliefs about reality, even when those beliefs are false.

In human developmental studies, it is only after age 4 that children pass traditional false-belief tests, in which they must explicitly predict a mistaken agent's future actions (*7*). However, recent evidence has shown that even young infants can pass modified false-belief tests that involve the use of simplified task procedures and spontaneous-gaze responses as measures [e.g., violation of expectation (*8*), anticipatory looking (*9*, *10*)]. For example, anticipatory looking paradigms exploit

[1]Department of Evolutionary Anthropology, Duke University, Durham, NC 27708, USA. [2]Kumamoto Sanctuary, Wildlife Research Center, Kyoto University, Kumamoto, Japan. [3]Primate Research Institute, Kyoto University, Inuyama, Japan. [4]School of Psychology and Neuroscience, University of St Andrews, St Andrews, UK. [5]Department of Developmental and Comparative Psychology, Max Planck Institute for Evolutionary Anthropology, Leipzig, Germany. [6]Department of Psychology and Neuroscience, Duke University, Durham, NC 27708, USA.
*These authors contributed equally to this work. **†Corresponding author. Email: ckrupenye@gmail.com (C.K.); fkanou@gmail.com (F.K.)**

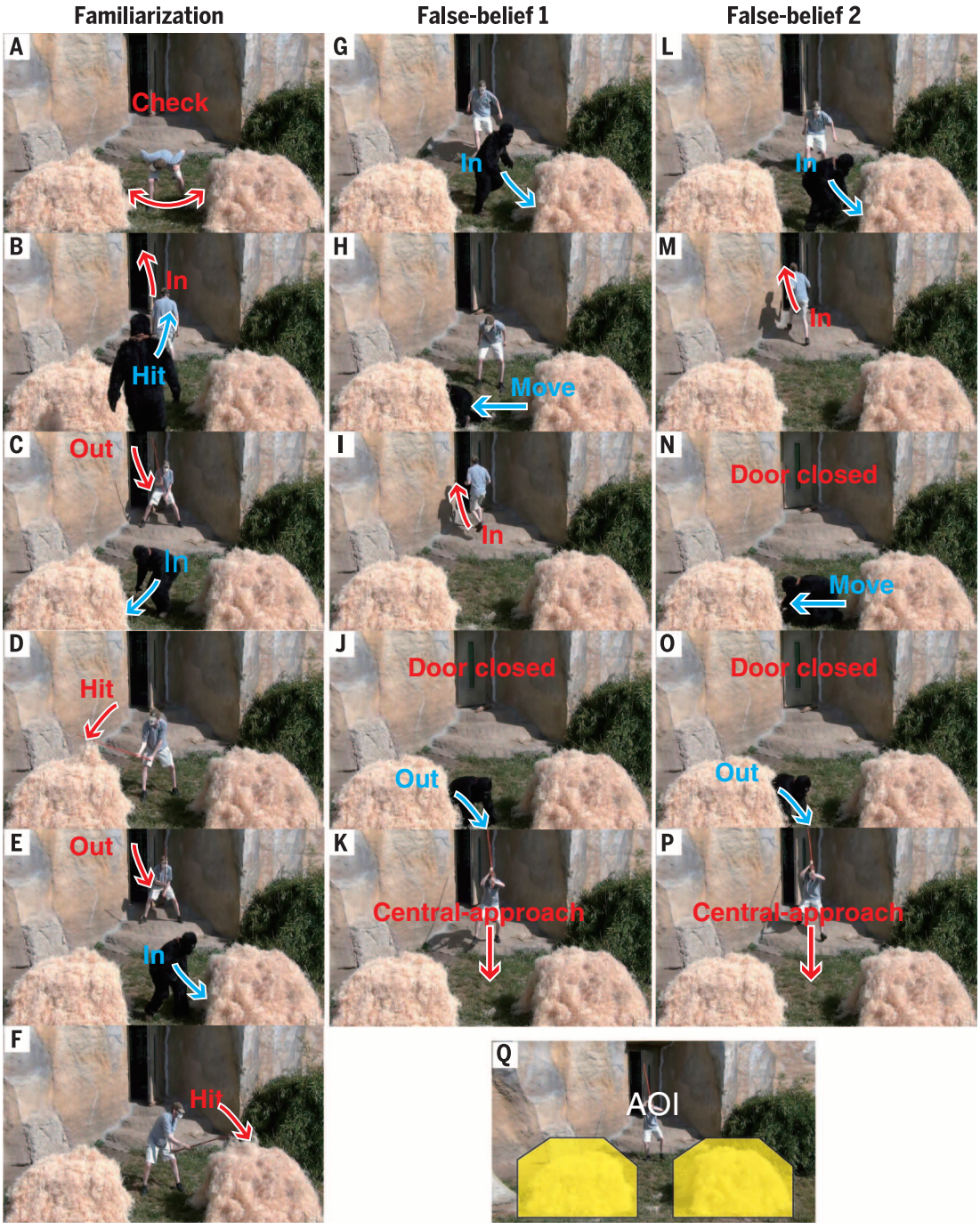

Fig. 1. Events shown in experiment one. (**A** to **F**) Familiarization. (**G** to **J**) Belief induction for the FB1 (false belief one) condition. (**K**) Central approach for FB1. (**L** to **O**) Belief induction for FB2. (**P**) Central approach for FB2. (**Q**) Areas of interest (AOIs) defined for the target and distractor haystacks. See movie S1.

individuals' tendency to look to a location in anticipation of an impending event and thus can measure a participant's predictions about what an agent is about to do, even when that agent holds a false belief about the situation. Only two studies have used spontaneous-gaze false-belief tasks with nonhuman primates. Both failed to replicate with monkeys the results with infants, despite monkeys' success in true-belief conditions (*11*, *12*).

In our study, we used an anticipatory looking measure (*10*) to test for false-belief understanding in three species of apes (chimpanzees, *Pan troglodytes*; bonobos, *Pan paniscus*; orangutans, *Pongo abelii*). Previous studies have established that apes reliably make anticipatory looks based on agents' goal-directed actions and subjects' event memories (*13*, *14*). In our experiments, apes watched short videos on a monitor while their gaze was noninvasively recorded using an infrared eye-tracker. Our design, controls, and general procedure replicated a seminal anticipatory looking false-belief study with human infants (*10*).

We conducted a pair of experiments using the same design but introduced distinct scenarios in each. The common design involved two familiarization trials followed by a single test trial [either the FB1 or FB2 (false belief one or two) condition; between-subjects design]. In our scenarios, a human agent pursued a goal object that was hidden in one of two locations. During the first familiarization, the agent witnessed the hiding of the object in one location before searching for it there. In the second, the object was hidden in the other location and the agent pursued it there. These trials served to demonstrate that the object could be hidden in either of the two locations and that, when knowledgeable, the agent would search for it in its true location. During the belief-induction phase, the agent witnessed the initial hiding of the object, but the object was then moved to a second location while the agent was either present

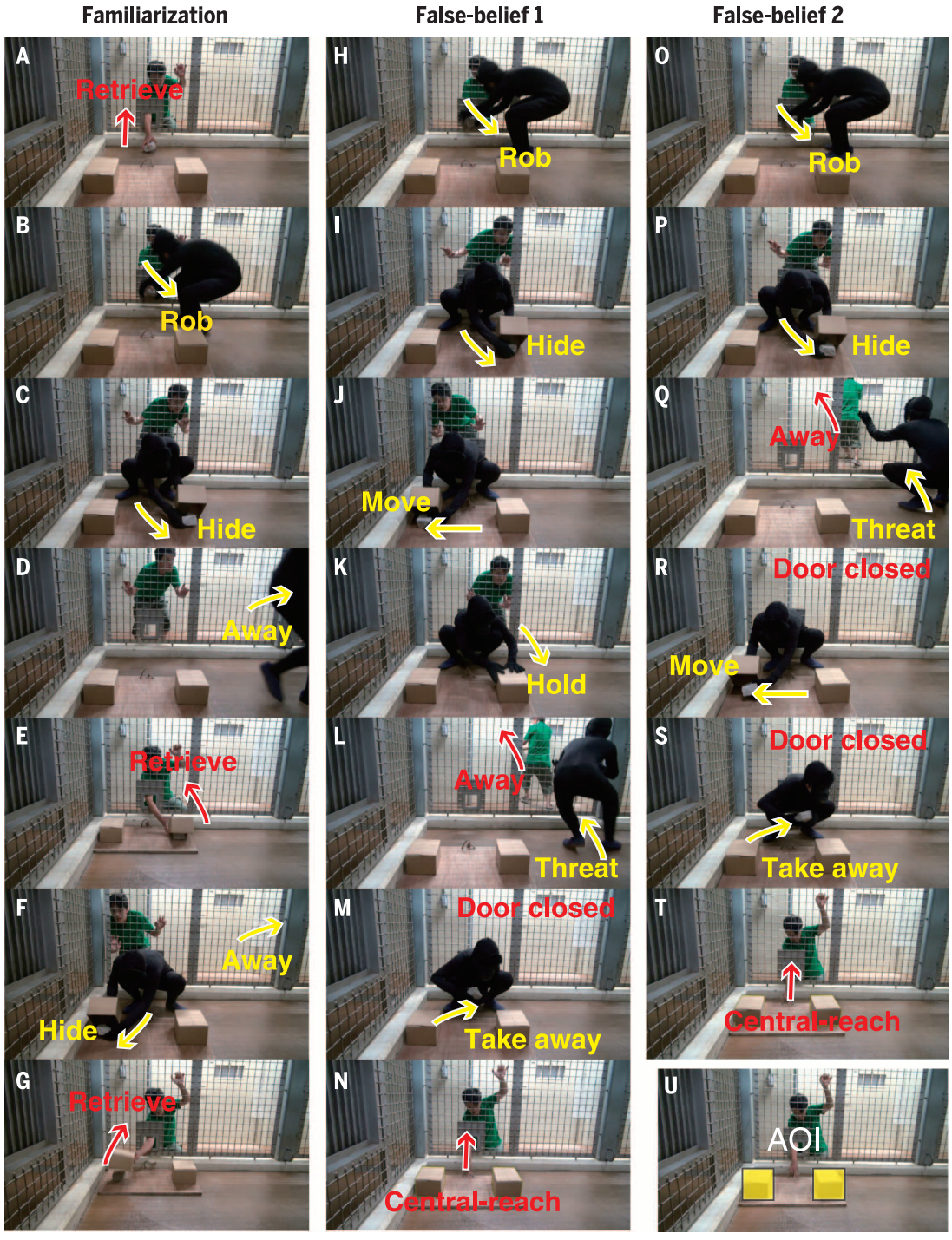

Fig. 2. Events shown in experiment two. (**A** to **G**) Familiarization. (**H** to **M**) Belief induction for the FB1 condition. (**N**) Central reach for FB1. (**O** to **S**) Belief induction for FB2. (**T**) Central reach for FB2. (**U**) AOIs defined for the target and distractor boxes. Following the infant study (*10*), we included an additional action in FB1 [KK touched the distractor box (K)] to control for subjects looking to the last place that the actor attended. See movie S2.

(FB1) or absent (FB2). In both conditions, the object was then completely removed before the agent returned to search for it. The actions presented during the induction phase controlled for several low-level cues—namely, that participants could not solve the task by simply expecting the agent to search in the first or last location where the object was hidden or the last location where the agent attended (*10*). Whether the object was hidden first in the left or right location during familiarization trials and whether the target of the agent's false belief was the left or right location during test trials were counterbalanced across subjects.

Experiments one and two presented scenarios that were specifically intended to evoke apes' spontaneous action anticipation in different contexts. To encourage subjects' engagement, we presented simulated agonistic encounters between a human (actor) and King Kong (KK), an unreal apelike character unfamiliar to the subjects (*14*). To minimize the possibility that apes could solve the task by responding to learned behavioral cues, our scenarios involved events that were novel to our participants. In experiment one, the actor attempted to search for KK, who had hidden himself in one of two large haystacks (Fig. 1 and movie S1). In experiment two, the actor attempted to retrieve a stone that KK had stolen and hidden in one of two boxes (Fig. 2 and movie S2). We confirmed that apes unambiguously attended to the depicted actions during the belief-induction phases of both experiments (figs. S3 and S4) (*15*).

Apes' anticipatory looks were assessed on the basis of their first looks to the target (the location where the actor falsely believed the object to be)

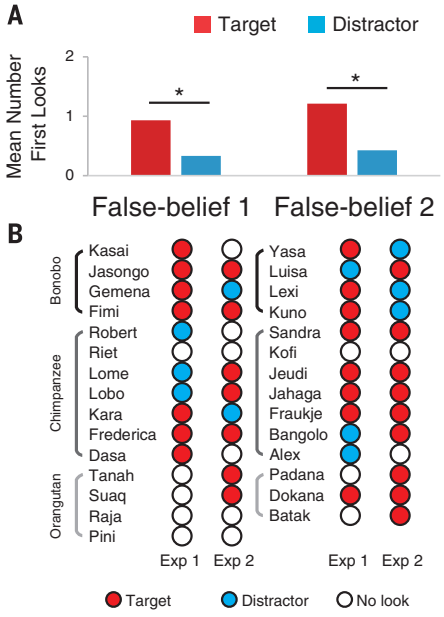

Fig. 3. Apes' performance across the two experiments. (**A**) Mean number of first looks to the target and the distractor for the 29 subjects who participated in both experiments. Asterisks indicate $P < 0.05$, Wilcoxon signed rank test. (**B**) Individual scores in each experiment.

Table 1. Number of participants who made first looks to either the target or the distractor during the agent's approach in experiments one ($N = 40$) and two ($N = 30$). Values in parentheses indicate the number of participants who did not look at either.

Condition	Target	Distractor	Total
	Experiment one		
FB1	10	4	14 (6)
FB2	10	6	16 (4)
Total	20	10	30 (10)
	Experiment two		
FB1	8	2	10 (6)
FB2	9	3	12 (2)
Total	17	5	22 (8)

or the distractor (the other location) as the actor ambiguously approached the two locations—from the start to the end of the actor's walk toward the haystacks [central approach; experiment one (Fig. 1, K and P)] and reach toward the boxes [central reach; experiment two (Fig. 2, N and T)] (both 4.5 s). Software scored looks automatically on the basis of areas of interest (*15*) (Figs. 1Q and 2U). The actor's gaze and gait during the central approach and central reach provided no directional cues (figs. S1 and S2) (*15*), and the videos ended without the actor hitting or grabbing the target. We used two different scenarios to gauge the robustness of apes' responses under different conditions.

Table 1 summarizes the results for each experiment. In experiment one, we tested 40 apes [19 chimpanzees, 14 bonobos, and 7 orangutans (table S1) (*15*)]. Thirty subjects looked to either the target or the distractor during the central-approach period. Of these 30, 20 looked first at the target ($P = 0.098$, two-tailed binomial test). There was no difference between the FB1 and FB2 conditions ($P = 0.70$, Fisher's exact test). In experiment two, we tested 30 subjects (29 from experiment one, plus one additional bonobo). Twenty-two apes made explicit looks to the target or the distractor during this period. Of these 22, 17 looked first at the target ($P = 0.016$, two-tailed binomial test), and there was no difference between the FB1 and FB2 conditions ($P = 1.0$, Fisher's exact test).

We then conducted a combined analysis with the 29 apes that participated in both experiments. We compared the number of first looks (maximum of two looks; i.e., one per experiment) each subject made to the target versus to the distractor during the central-approach and central-reach periods (Fig. 3). Apes made significantly more first looks to the target than to the distractor, both overall (Wilcoxon signed rank test: $Z = 3.25$, $N = 29$, $P = 0.001$, $r = 0.42$) and in each condition (FB1: $Z = 1.98$, $N = 15$, $P = 0.046$, $r = 0.36$; FB2: $Z = 2.15$, $N = 14$, $P = 0.031$, $r = 0.40$) (Fig. 3A). No significant difference was detected across species. To test this, we first calculated difference scores for each ape (number of first looks to target minus to distractor) and then subjected these scores to the Kruskal-Wallis H test [$\chi^2(2) = 0.46$, $P = 0.79$] (Fig. 3B).

Our findings show that apes accurately anticipated the goal-directed behavior of an agent who held a false belief. Our design and results controlled for several explanations. First, apes could not solve the task by simply expecting the actor to search in the first or last location where the object was hidden, the last location the actor attended, or the last location KK acted on. Second, apes could not merely respond to violations of three-way associations between the actor, the target object, and the object's location, formed during familiarization or belief-induction phases (*16*). Instead, the apes actively predicted the actor's behavior. Heyes (*17*) argued that a low-level account could explain Southgate *et al.*'s (*10*) results if subjects overlooked the object's movement while the agent was not attending and imagined the object in its previous location. We confirmed that apes closely tracked all such movements (figs. S3 and S4) (*15*). Third, our results cannot be explained as attribution of ignorance rather than false belief. Apes did not simply expect the actor's ignorance to lead to error or uncertainty (*18*); they specifically anticipated that the actor would search for the object where he falsely believed it to be.

Apes were never shown the actor's search behavior when he held a false belief, precluding reliance on external behavioral cues learned during the task. By requiring subjects to make predictions in situations that involved a constellation of novel features (e.g., a human attacking an apelike character hiding in a haystack), we also minimized the possibility that subjects could apply behavior rules acquired through extensive learning during past experiences. Nevertheless, we acknowledge that all change-of-location false-belief tasks are, in principle, open to an abstract behavior rule–based explanation—namely, that apes could solve the task by relying on a rule that agents search for things where they last saw them (*16*). However, this explanatory framework cannot easily accommodate the diversity of existing evidence for ape TOM (*3*) nor can it account for recent evidence that human infants and apes appear to infer whether others can see through objects that look opaque, based on their own experience with the occlusive properties (i.e., see-through or opaque) of those objects (*19*, *20*).

Thus, our results, in concert with existing data, suggest that apes solved the task by ascribing a false belief to the actor, challenging the view that the ability to attribute reality-incongruent mental states is specific to humans. Given that apes have not yet succeeded on tasks that measure false-belief understanding based on explicit behavioral choices (*4*–*6*), the present evidence may constitute an implicit understanding of belief (*9*). Differential performance between tasks may reflect differences in task demands or context, or less flexible abilities in apes compared with humans. At minimum, apes can anticipate that an actor will pursue a goal object where he last saw it, even though the apes themselves know that it is no longer there. That great apes operate, at least on an implicit level, with an understanding of false beliefs suggests that this essential TOM skill is likely at least as old as humans' last common ancestor with the other apes.

REFERENCES AND NOTES

1. D. Premack, G. Woodruff, *Behav. Brain Sci.* **1**, 515–526 (1978).
2. R. W. Byrne, A. W. Whiten, *Machiavellian Intelligence: Social Expertise and the Evolution of Intellect in Monkeys, Apes, and Humans* (Clarendon Press, 1988).
3. J. Call, M. Tomasello, *Trends Cogn. Sci.* **12**, 187–192 (2008).
4. B. Hare, J. Call, M. Tomasello, *Anim. Behav.* **61**, 139–151 (2001).
5. J. Kaminski, J. Call, M. Tomasello, *Cognition* **109**, 224–234 (2008).
6. C. Krachun, M. Carpenter, J. Call, M. Tomasello, *Dev. Sci.* **12**, 521–535 (2009).
7. H. M. Wellman, D. Cross, J. Watson, *Child Dev.* **72**, 655–684 (2001).
8. K.H. Onishi, R. Baillargeon, *Science* **308**, 255–258 (2005).
9. W. A. Clements, J. Perner, *Cogn. Dev.* **9**, 377–395 (1994).

10. V. Southgate, A. Senju, G. Csibra, *Psychol. Sci.* **18**, 587–592 (2007).
11. D. C. Marticorena, A. M. Ruiz, C. Mukerji, A. Goddu, L. R. Santos, *Dev. Sci.* **14**, 1406–1416 (2011).
12. A. Martin, L. R. Santos, *Cognition* **130**, 300–308 (2014).
13. F. Kano, J. Call, *Psychol. Sci.* **25**, 1691–1698 (2014).
14. F. Kano, S. Hirata, *Curr. Biol.* **25**, 2513–2517 (2015).
15. Materials and methods are available as supplementary materials on *Science* Online.
16. J. Perner, T. Ruffman, *Science* **308**, 214–216 (2005).
17. C. Heyes, *Dev. Sci.* **17**, 647–659 (2014).
18. R. Baillargeon, R. M. Scott, Z. He, *Trends Cogn. Sci.* **14**, 110–118 (2010).
19. A. Senju, V. Southgate, C. Snape, M. Leonard, G. Csibra, *Psychol. Sci.* **22**, 878–880 (2011).
20. K. Karg, M. Schmelz, J. Call, M. Tomasello, *Anim. Behav.* **105**, 211–221 (2015).

ACKNOWLEDGMENTS

We thank the staff at the Wolfgang Kohler Primate Research Center and Kumamoto Sanctuary for assistance. Financial support was provided by the NSF Graduate Research Fellowship Program (grant DGE-1106401 to C.K.), the Ministry of Education, Culture, Sports, Science and Technology of Japan (grant K-CONNEX to F.K.), the Japan Society for the Promotion of Science (grants KAKENHI 26885040 and 16K21108 to F.K. and grants KAKENHI 26245069 and 24000001 to S.H.), and the European Research Council (Synergy grant 609819 SOMICS to J.C.). Data are available in the main text and supplementary materials.

SUPPLEMENTARY MATERIALS

www.sciencemag.org/content/354/6308/110/suppl/DC1
Materials and Methods
Supplementary Text
Figs. S1 to S5
Tables S1 to S5
Movies S1 and S2

27 April 2016; accepted 26 August 2016
10.1126/science.aaf8110

STRUCTURAL BIOLOGY

The methanogenic CO_2 reducing-and-fixing enzyme is bifunctional and contains 46 [4Fe-4S] clusters

Tristan Wagner,[1] Ulrich Ermler,[2] Seigo Shima[1,3]*

Biological methane formation starts with a challenging adenosine triphosphate (ATP)–independent carbon dioxide (CO_2) fixation process. We explored this enzymatic process by solving the x-ray crystal structure of formyl-methanofuran dehydrogenase, determined here as Fwd(ABCDFG)$_2$ and Fwd(ABCDFG)$_4$ complexes, from *Methanothermobacter wolfeii*. The latter 800-kilodalton apparatus consists of four peripheral catalytic sections and an electron-supplying core with 46 electronically coupled [4Fe-4S] clusters. Catalysis is separately performed by subunits FwdBD (FwdB and FwdD), which are related to tungsten-containing formate dehydrogenase, and subunit FwdA, a binuclear metal center carrying amidohydrolase. CO_2 is first reduced to formate in FwdBD, which then diffuses through a 43-angstrom-long tunnel to FwdA, where it condenses with methanofuran to formyl-methanofuran. The arrangement of [4Fe-4S] clusters functions as an electron relay but potentially also couples the four tungstopterin active sites over 206 angstroms.

Methanogenic archaea produce ~1 billion tons of methane per year and thus play an important ecological role in the global carbon cycle (*1*). Biological methane is produced mainly from acetate and CO_2-H_2 (*1*). For methanogenesis from CO_2, the metabolic pathway starts with the reduction of CO_2 to form formyl-methanofuran (formyl-MFR) (E_0' = −530 mV, where E_0' is the standard redox potential at pH 7) (*2*), using reduced ferredoxin (E' = ~−500 mV, where E' is a physiological redox potential at pH 7) (*1*) as the electron donor (Fig. 1A). The reaction is catalyzed by formyl-MFR dehydrogenase. There are two isoenzymes in most methanogens, a tungsten iron-sulfur protein (Fwd) and a molybdenum iron-sulfur protein (Fmd) (*3*–*9*).

Formyl-MFR dehydrogenase uses CO_2 rather than bicarbonate as a substrate (*10*, *11*). CO_2 spontaneously reacts with MFR to form carboxy-MFR at a rate that is compatible with carboxy-MFR being an intermediate in CO_2 reduction to formyl-MFR (*10*, *11*). Therefore, it was assumed that carboxy-MFR is reduced to formyl-MFR in a subsequent step at the tungsten or molybdenum active site of formyl-MFR dehydrogenases. This reaction sequence is in line with all other CO_2-fixing enzymatic processes, except for that of acetogenesis, where CO_2 is first reduced to formate and then conjugated with N-10 of tetrahydrofolate using adenosine triphosphate (ATP) (*12*).

To elucidate the catalytic mechanism of this sequence, we purified and crystallized the tungstopterin-containing formyl-MFR dehydrogenase (FwdABCDFG) complex from the thermophilic methanogenic archaeon *Methanothermobacter wolfeii* (fig. S1) under strict anoxic conditions in four crystal forms (table S1) (*13*). The x-ray analysis of individual subunit structures and, subsequently, of the whole protein complex is primarily based on orthorhombic and triclinic crystals diffracting to 1.9 and 2.6 Å resolution, in which the enzyme is present as a dimer of the FwdABCDFG heterohexamer [12-subunit oligomer (12-mer)] (Fig. 1B and fig. S2A) and a tetramer of the heterohexamer (24-mer) (fig. S2B), respectively. Notably, FwdF and FwdG were absent in gel electrophoresis but are integral components of the enzyme complex.

Subunit FwdA (63 kDa) is structurally classified as a member of the amidohydrolase superfamily, which includes urease, phosphotriesterase, dihydroorotase, and dihydropyrimidinases (fig. S3) (*7*–*9*). These enzymes are characterized by a binuclear metal center positioned inside a deep solvent-accessible cavity at the entry of an $(\alpha/\beta)_8$ TIM barrel. The metal center is predicted to be composed of two zinc atoms that are analogous to the most structurally related enzyme, dihydroorotase (*14*). FwdA also contains zinc ligands, N6-carboxylysine, and a catalytically crucial aspartate, all of which are strictly conserved in the amidohydrolase superfamily (Fig. 2D and figs. S3A and S4). The x-ray structure of the triclinic 24-mer crystals soaked with MFR revealed the bulky C1 carrier in the cavity between the dinuclear metal center and the bulk solvent (Fig. 2D and fig. S4).

Subunit FwdB (48 kDa) harbors the tungstopterin active site and a [4Fe-4S] cluster. This subunit is structurally related to domains I, II, and III of molybdenum- and tungsten-containing formate dehydrogenase (*7*–*9*); FwdD (14 kDa) is structurally related to domain IV (*7*–*9*). A solution nuclear magnetic resonance structure of FwdD from *Archaeoglobus fulgidus* has been reported (Protein Data Bank ID: 2KI8). The redox-active tungsten of FwdBD (FwdB and FwdD) is coordinated by four dithiolene thiolates of two tungstopterin guanine dinucleotide molecules (Fig. 2, A to C), by the thiolate of Cys^{118}, and by an inorganic sulfido ligand (fig. S5). The residues involved in the [4Fe-4S] cluster, pterin-binding, tungsten-ligation, and active sites are essentially conserved between FwdBD and the molybdenum- or tungsten-containing formate dehydrogenases (*15*–*18*). FwdC (29 kDa) is a subunit with low sequence similarity to the C-terminal domain of glutamate synthase (*19*), flanking the tunnel that channels ammonia between the two active sites.

FwdF (39 kDa) is a polyferredoxin composed of four similar ferredoxin domains (*7*–*9*) that are arranged in a T-shaped conformation (Fig. 1C and figs. S6 and S7). The fusion of the ferredoxin domains, each carrying two [4Fe-4S] clusters, does not occur consecutively; the third ferredoxin domain (amino acids 143 to 221) is inserted into the second ferredoxin domain (amino acids 106 to 137 and 228 to 257) (fig. S7A). FwdG (8.6 kDa) adopts a classical ferredoxin fold that hosts two [4Fe-4S] clusters.

The 12-mer has an electron-supplying core (two FwdFG subunits) and two flanking catalytic sections, each formed by FwdA and FwdBD.

[1]Max Planck Institute for Terrestrial Microbiology, Karl-von-Frisch-Straße 10, 35043 Marburg, Germany. [2]Max Planck Institute of Biophysics, Max-von-Laue-Straße 3, 60438 Frankfurt am Main, Germany. [3]Precursory Research for Embryonic Science and Technology (PRESTO), Japan Science and Technology Agency (JST), 332-0012 Saitama, Japan.
*Corresponding author. Email: shima@mpi-marburg.mpg.de